Brain Struct Funct
DOI 10.1007/s00429-017-1471-6

ORIGINAL ARTICLE

Topography of the human acoustic radiation as revealed by ex vivo fibers micro-dissection and in vivo diffusion-based tractography

Chiara Maffei[1] · Jorge Jovicich[1] · Alessandro De Benedictis[2] · Francesco Corsini[3] · Mattia Barbareschi[4] · Franco Chioffi[3] · Silvio Sarubbo[3]

Received: 11 April 2017 / Accepted: 4 July 2017

Abstract The acoustic radiation is a compact bundle of fibers conveying auditory information from the medial geniculate nucleus of the thalamus to the auditory cortex. Topographical knowledge of this bundle in primates is scarce and in vivo diffusion-based tractography reconstructions in humans remains challenging, especially with the most widely used MRI acquisition protocols. Therefore, the AR represents a notable anatomical omission in the neurobiological investigation of acoustic and linguistic functional mechanisms in humans. In this study, we combine blunt micro-dissections and advanced diffusion tractography methods to provide novel insights into the topographical anatomy of this bundle in humans. Evidences from ex vivo blunt micro-dissection in three human (two right) hemispheres are compared to the 3D profile of this bundle as reconstructed by tractography techniques in four healthy adult data sets provided by the Human Connectome Project. Both techniques show the unique trajectory of the AR, a transversal course from the midline to the lateral convexity of the posterior temporal lobe. Blunt dissections demonstrated three portions of this bundle that we defined as the genu, stem, and fan, revealing the intimate relationships that each of these components has with neighboring association and projection pathways. Probabilistic tractography and ultra-high *b* values provided results comparable to blunt micro-dissections and highlighted the main limitations in tracking the AR. This is, to our knowledge, the first ex vivo/in vivo integrated study providing novel and reliable information about the precise anatomy of the AR, which will be important for future investigations in the neuroscientific, clinical, and surgical field.

Keywords Acoustic radiation · Diffusion tractography · Post-mortem dissection · Auditory tract · Auditory pathways

Introduction

The acoustic radiation (AR) constitutes a major sensory projection pathway, transferring primary auditory information from the medial geniculate nucleus (MGN) of the thalamus on the auditory cortex to the transverse temporal gyrus of Heschl (HG).

The connectivity pattern of these fibers has been described in some detail in cytoarchitectonic and myeloarchitectonic studies in non-human primates (Mesulam and Pandya 1973; Hackett et al. 1998) and to some extent in humans (Tardif and Clarke 2001). These studies mainly provide information on connectivity aspects between the MGN and the auditory projection cortical territory and little emphasis was given to the anatomy of

Electronic supplementary material The online version of this article (doi:10.1007/s00429-017-1471-6) contains supplementary material, which is available to authorized users.

✉ Silvio Sarubbo
silviosarubbo@gmail.com

[1] CIMeC Center for Mind/Brain Sciences, Trento University, Trento, Italy

[2] Neurosurgery Unit, Department of Neuroscience and Neurorehabilitation, Bambino Gesù Children's Hospital, IRCCS, Rome, Italy

[3] Division of Neurosurgery, Structural and Functional Connectivity Lab (SFC-LSB) Project, Department of Neurosciences, "S. Chiara" Hospital, Trento APSS, 9, Largo Medaglie d'Oro, 38122 Trento, Italy

[4] Department of Histopathology, "S. Chiara" Hospital, Trento APSS, Trento, Italy

Published online: 02 September 2017

the tract itself. To a more macro-anatomical level, Bürgel et al. (2006) described the trajectory of this bundle from the MGN to the cortex. However, still, very little is known about its topography and, in particular, its relationship with adjacent white matter (WM) bundles. Most of the available information about the anatomy of the AR traces back to the pioneering work of the anatomists of the 19th and early 20th century, who used gross dissection, myelin staining, and lesion degeneration methods to investigate AR topography. These early reports described the AR as a compact bundle of fibers leaving the MGN and pursuing an antero-lateral direction passing through the posterior portion of the internal capsule, proceeding along the corona radiata, curving around the inferior sulcus of the insula before reaching the transverse temporal HG (Dejerine 1895; Flechsig 1920; Pfeifer 1920). While being of undeniable value, these old maps lack fine anatomo-topographical details and have limited value as references in neuroimaging studies.

Over the past decade, diffusion tractography techniques have emerged as the main tool for the investigation of the WM architecture in vivo (Catani et al. 2002; Tournier et al. 2011). However, it is still challenging to perform diffusion-based reconstructions of the AR (Maffei et al. 2015) using the most widespread MRI acquisition protocols and standard processing pipelines. As a result, the AR is missing from most tractography studies investigating auditory processing and the integration of language and non-language auditory inputs, as well as from diffusion-based atlases (Thiebaut de Schotten et al. 2011). The main challenges in reconstructing the trajectory of the AR are related to the intrinsic anatomical features of these projection fibers: short tract length; small dimensions; atypical medio-lateral course; dense fiber crossing with projection; and association fibers. The inability to completely solve multiple fibers orientations inside the voxel constitutes one of the main limitations of tractography (Jeurissen et al. 2013). Compared to the classic tensor model (Basser et al. 1994), new algorithms, such as constrained spherical deconvolution (CSD), have been developed to improve this reconstruction issue (Dell'Acqua et al. 2010; Tournier et al. 2008). However, these methods can still provide inaccurate or ambiguous descriptions of local fiber orientations and thus unreliable 3D reconstructions, in regions with very complex fiber architectures and high density of crossing (Jones and Cercignani 2010). Using multi-fiber models and probabilistic tractography algorithms, few studies have been able to recover the 3D profile of the AR (Behrens et al. 2007; Crippa et al. 2010; Berman et al. 2013; Javad et al. 2014). Nevertheless, AR reconstruction is variable across these studies, and no detailed topographical descriptions are provided. Clear topographical information on the course of these fibers from the MGN to the HG and on their relationship with neighboring WM bundles is missing or only hypothesized on the base of studies on monkeys.

In this scenario, validation of tractography results is crucial. The spreading of diffusion-based tractography techniques has, therefore, renewed the interest in blunt micro-dissections of human WM (Martino et al. 2010; Wang et al. 2012; Fernández-Miranda et al. 2015; Sarubbo et al. 2015; De Benedictis et al. 2016; Wang et al. 2016; Sarubbo et al. 2016). The unique information provided by blunt micro-dissections on the trajectory and topographical organization of the WM bundles constitute a baseline by which the methodological process can be improved to overcome the limits of tractography reconstructions.

Successful and reliable reconstructions of the AR will be crucial for neuroscientific, clinical, and surgical applications. Robust AR reconstruction in vivo could help case–control studies in pathological groups, but also would allow for the identification of the left–right asymmetries and functional mechanisms sub-served by this bundle, that are currently unknown. In particular, evaluating the mechanisms of the anatomo-functional relations of this tract would help to shed a light on the neural basis of language comprehension, contributing to enhance the cornerstone model of language processing (Hickok and Poeppel 2007; Poeppel et al. 2012). Moreover, reliable tractographic reconstruction of the AR will support neuropsychological, clinical, and surgical applications.

In this study, we combine blunt micro-dissection and advanced diffusion imaging tractography methods with the following goals: (1) to provide, for the first time to our knowledge, a detailed and multimodal anatomical description of the trajectory and terminations of the AR in humans and (2) to characterize the topography of this bundle in respect to the other neighboring tracts. Results obtained with ex vivo dissections and in vivo tractography are compared and integrated, and limitations discussed.

Materials and methods

Fiber dissection

Three human cerebral hemispheres (two right) were prepared according to the modified Klinger's preparation previously described (Sarubbo et al. 2015, 2016). Micro-dissection (5×) was performed by an expert anatomist and neurosurgeon (the senior author, S.S.). The AR was approached posteriorly starting a layer-by-layer dissection from the posterior third of the superior temporal sulcus (STS) and its elongation in the inferior parietal lobe (IPL) (Sarubbo et al. 2016). U-fibers connecting the supra-marginal gyrus (SMG) and the angular gyrus (AG) with the cortices of the posterior two-thirds of the STS were

removed (Fig. 1a). The stem of the vertical indirect posterior portion of the superior longitudinal fasciculus (SLF) was highlighted and cut (Fig. 1b), demonstrating the temporal portion of the arcuate fascicle (AF) (Fig. 1c). The deepest portion and the most ventral fibers of the AF, connecting the frontal lobe to the posterior third of STG (Fig. 1d), were removed to highlight the posterior thalamic radiation (PTR) and the AR fibers projecting to HG. The AR was progressively defined in a medio-lateral direction, preserving portions of neighboring projection [posterior thalamic radiation (PTR); external capsule (EC); and internal capsule (IC)] and association (AF and SLF)] fibers.

Tractography

Diffusion and structural data of four healthy adult subjects provided by the Human Connectome Project database were analyzed using MrTrix (Tournier et al. 2012). Data were previously preprocessed as described in Fan et al. (2015). The HARDI multi-shell data set is composed of four shells (1000–3000–5000–10000 s/mm^2) for a total of 552 directions at an isotropic spatial resolution of 1.25 mm. A multi-shell multi-tissue constrained spherical deconvolution algorithm (Jeurissen et al. 2014) was fit to the data and anatomically constrained (Smith et al. 2012) probabilistic tractography was performed using the following parameters: 0.75 mm step-size, 45° angle threshold, and 1000 seeds/voxel. The structural T1-weighted image of each subject was registered to the diffusion space using the up-sampled fractional anisotropy map in ANTS (Klein et al. 2009). After registration, the T1-weighted image of each subject was segmented in FSL using FAST (Zhang et al. 2001) and FIRST (Patenaude et al. 2012) to create a five-tissue-type image to be used for anatomically constrained

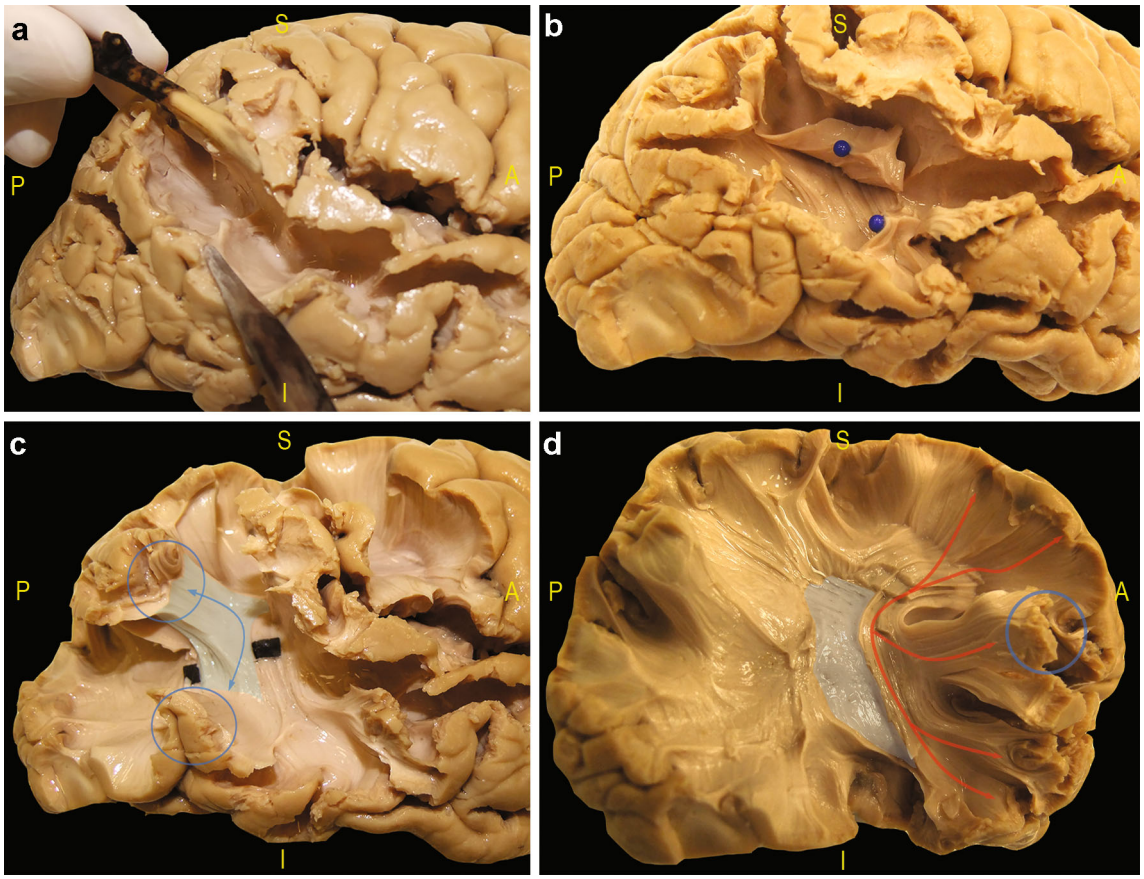

Fig. 1 Layer-by-layer dissection of the AR. **a** Removal of the compact and homogeneous layer of U-fibers connecting the IPL to the posterior third of STS (the decorticated area at the center of the anatomical scene of this panel). **b** In this panel, we demonstrate and cut the stem of the indirect posterior component of the SLF, lifted up by two blue pins at the two extremities of the cut. **c** In a deeper layer, we demonstrate the Wernicke's fascicle (highlighted in *light blue*, with *blue arrows* and *circles* showing the main fibers course and terminations, respectively). This bundle is just more superficial and posterior to the layer of AF stem, highlighted in this picture by the *black tag*. **d** Finally, after removal of Wernickes' fascicle, we completely expose the course of the AF (*red arrows*), running above the EC (*light blue*). We highlight its terminations in the most posterior portion of STG (*blue circle*), bordering the posterior portion of the middle third of the AR fibers. *AF* arcuate fascicle, *AR* acoustic radiation, *EC* external capsule, *IPL* inferior parietal lobule, *SLF* superior longitudinal fascicle, *STG* superior temporal gyrus, *STS* superior temporal sulcus

tractography (ACT) (Smith et al. 2012). The left and right thalamus were segmented in FSL using FIRST on each subject's T1 and the HG was carefully manually defined in each subject's hemisphere by the same operator (first author, C.M.). Tractography was randomly initiated from every voxel in the thalamus and HG was used as including region: only streamlines leaving the thalamus and passing through HG were retained. To qualitatively evaluate the robustness of the tractography results, the reverse seeding strategy was also performed: tractography was randomly initiated from every voxel in the HG ROI and the thalamus was used as including ROI.

To investigate the spatial relationship of the AR with adjacent association and projection tracts, whole brain tractography was also performed in one subject using the following parameters: 0.75 mm step-size, 45° angle threshold, and 10 seeds/voxel. Tractography was initiated from every voxel in a white matter brain mask segmented in FSL using FAST. From these data, using either one or two region of interest (ROI) approach (Catani et al. 2003, 2005), the streamlines of the posterior thalamic radiation (PTR), the arcuate fasciculus (AF), the internal capsule (IC), the external capsule (EC), and the inferior longitudinal fasciculus (ILF) were virtually dissected in FiberNavigator (Chamberland et al. 2014). For the PTR streamlines, the segmented thalamus and a big ROI encompassing the white matter of the occipital and parietal lobe were used. For the AF streamlines, an ROI was defined to encompass the fibers lateral to the corona radiate and medial to the cortex as previously described (Catani et al. 2002). To dissect the anterior indirect SLF streamlines, a first ROI was placed on the inferior frontal gyrus and a second one in the anterior parietal cortex. To dissect the posterior indirect SLF streamlines, an ROI was placed on the posterior middle temporal gyrus and a second ROI on the posterior portion of the inferior parietal lobe. To reconstruct the IC streamlines, a single ROI was placed around its posterior arm. For the EC streamlines, an ROI is defined on the axial slice around the white matter of the external capsule, and for the ILF streamlines, the occipital lobe ROI was used and a second ROI was placed in the white matter of the temporal pole.

Results

Trajectory and anatomical features

After removal of the ventral fibers of the AF, we exposed a texture of vertical and transverse fibers. Medially, we followed the compact and vertical layer of the projections fibers running from the thalamus to the post-central cortex. Antero-laterally to the stem of the AF, we exposed a transverse layer of fibers belonging to the AR, starting from the postero-lateral portion of the thalamus (MGN) (Fig. 2a). Blunt micro-dissections demonstrated a typical course of the AR, where three main distinct portions of the AR are visible. The proximal portion of the AR is characterized by a postero-lateral arching course. Middle portion of the AR fibers run in an antero-lateral direction, fanning out in the distal portion up to the whole cortex of HG. We defined these three portions as the genu, stem, and fan. The genu represents the most critical portion during the AR exposition. In this region, we observed how the AR densely intermingle with the vertical fibers projecting to the somato-sensory cortex (anterior part of the PTR), with the IC fibers and the posterior part of the PTR (Figs. 2, 3). The stem is located just in front of the AF stem, bordered posteriorly the postero-superior margin of the circular sulcus of the insula (Fig. 3c). The fan constitutes the roof of the WM of the posterior third of the temporal lobe.

Ultra-high *b* value and CSD tractography allowed for clear reconstruction of the AR profile in both hemispheres in all four subjects (Fig. 4). In accordance with blunt micro-dissections and previous literature (Bürgel et al. 2006), these streamlines occur as a compact bundle at the level of the MGN and extend along a postero-lateral (genu) and antero-lateral (stem and fun) direction, fanning out in the gray matter of HG (Fig. 4). On the coronal plane, we appreciated a straight medio-lateral projection of these fibers between the thalamus and the cortex. Tractography reconstructions confirmed the regions connected by this bundle are located on the same plane and highlighted that there is a typical S-shape course (Bürgel et al. 2006), due to AR fibers arching around the postero-superior portion of the circular sulcus of the insula.

Anatomical relationships with neighboring pathways

Results of in vivo tractography and ex vivo dissections showed the intricate anatomical relationships of the AR with the other bundles of this region. Over the whole trajectory between the MGN to HG, the AR fibers cross major association and projection pathways of the human brain, and are in close proximity with others (Figs. 2, 3). In the proximal portion, both techniques confirmed the strong intermingling between the AR running in a lateral direction and the vertical fibers of IC and PTR (Fig. 2a, b), including those projecting to the somato-sensory cortex. The middle third of the AR runs anteriorly to the AF stem, below the ventral portion of the fronto-parietal course of the AF and the anterior indirect SLF (also known as SLF III). Anteriorly to the AR, we highlighted, from the medial to lateral: IC fibers, EC fibers, claustro-opercular sub-insular fibers,

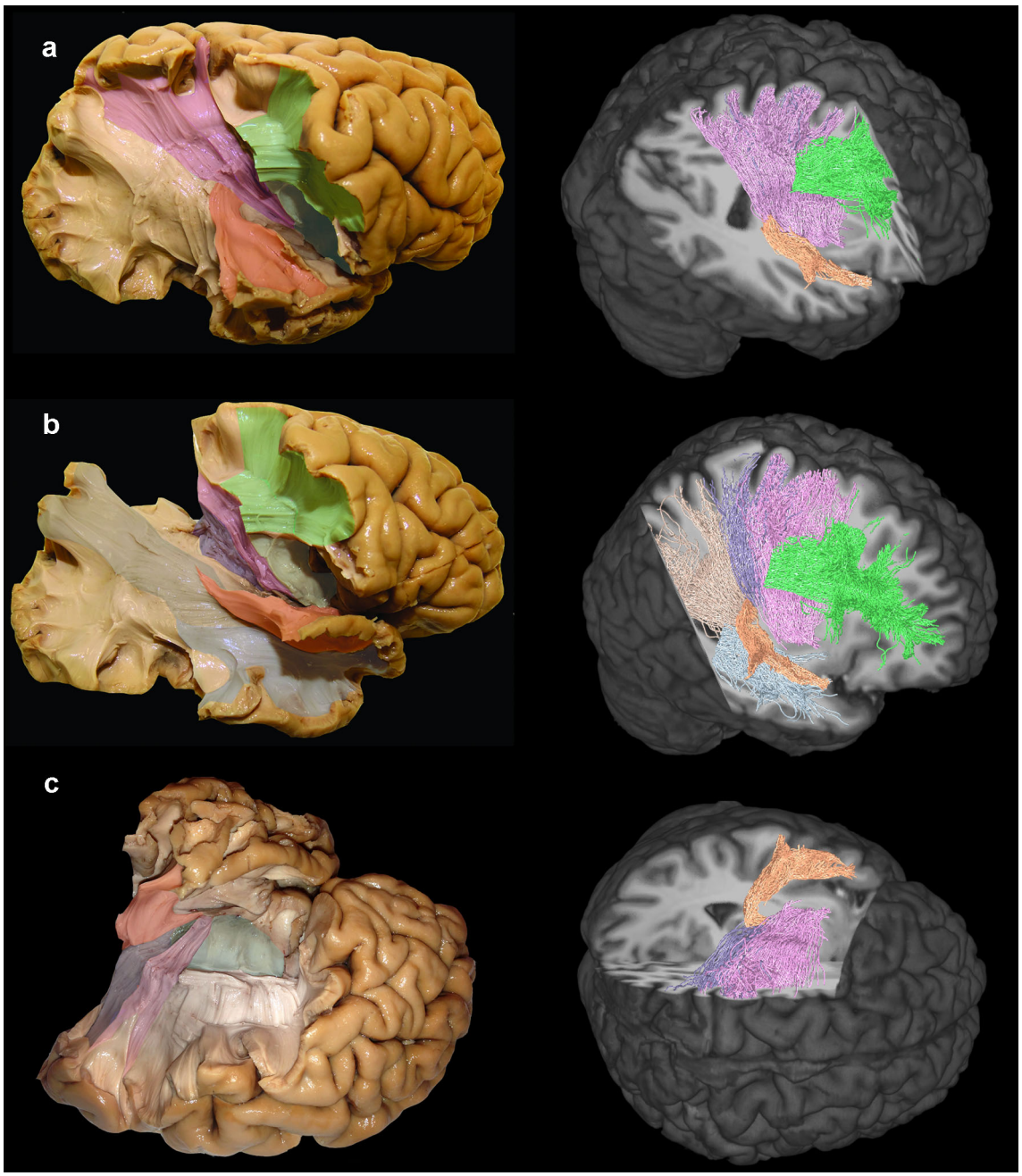

Fig. 2 Results from post-mortem micro-dissections and 3D tractography reconstructions. **a** Full latero-anterior arching course of AR (*orange*) is demonstrated from the postero-lateral thalamus to the cortex of the HG. The close relationship with the vertical fibers of the EC (*pink*) and AF (*green*) is shown. **b** Different layers of WM crossing the course of the AR at the parieto-temporal junction are shown, including: the horizontal fibers of the AF/SLF (indirect anterior portion) complex (*green*); the vertical fibers of the EC (*pink*); the fibers of the PTR (*light brown*), strongly intermingled with the proximal portion of the AR; and the dorsal portion of the ILF (*light blue*), bordering inferiorly the fan of AR. **c** Superior view of a left hemisphere showing the relationship between the AR (*orange*) and internal (*purple*) and external (*pink*) capsule fibers. *AF* arcuate fascicle, *AR* acoustic radiation, *EC* external capsule, *HG* Heschl gyrus, *IC* internal capsule, *ILF* inferior longitudinal fascicle, *SLF* superior longitudinal fascicle, *PTR* posterior thalamic radiation, *WM* white matter

and the insular cortices and posteriorly, from medial to lateral: the PTR fibers (including the optic radiation), the ILF, the AF, and the indirect posterior portion of the SLF (Figs. 2, 3). When comparing tractography results, AR terminations appear to be in close proximity (anterior and above) to the terminations of the most ventral streamlines of the AF, indirect anterior SLF, and indirect posterior SLF in the posterior third of STG and SMG (Fig. 3d, e).

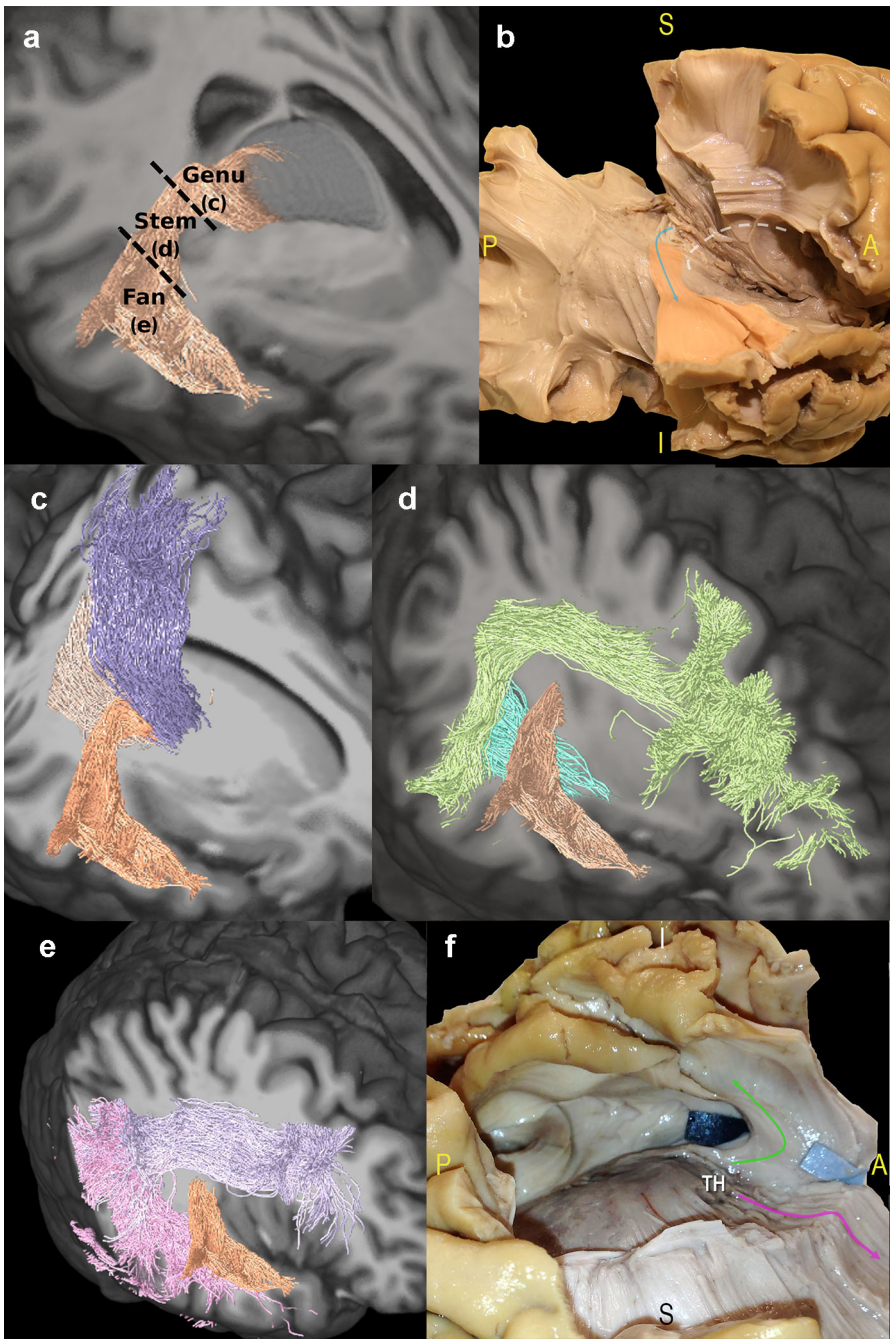

Fig. 3 Three portions of the AR—genu, stem, and fan—and their relationships with neighboring WM bundles. **a**, **b** Three portions of the AR are shown on the 3D tractography reconstruction of a representative subject (**a**) and on a dissected brain (**b**). In both panels, AR course is colored in pink. In the tractography reconstruction labels, defining the three portions of AR course (genu, stem, and fan) is showed. In the dissection image, a *white dotted line* highlights the superior and postero-superior courses of the circular sulcus of the insula. **c**–**e** Panels show the details of the relationships of the three portions with the other pathways. From *left* to *right*, **c** fibers of the genu are intermingled with the fibers of PTR (*light brown*) and, particularly, with the thalamic fibers projecting to the somatosensorial cortex (*purple*); **d** stem is close to the AF (*green*) and ILF (*light blue*); and **e** fan is very close to the terminations fibers of the indirect anterior SLF (*violet*) and indirect posterior portion of SLF (*pink*). **f** We show the emergence of the PTR (*purple arrow*) and the AR (*green arrow*) from the thalamus (TH). The fibers are separated by a *blue tag*, highlighting the dense crossing present at this level. The intermingling of vertical and transversal directions makes very hard to distinguish between these two contingents of fibers at their origin from the thalamus. *AF* arcuate fascicle, *AR* acoustic radiation, *ILF* inferior longitudinal fascicle, *PTR* posterior thalamic radiation, *SLF* superior longitudinal fascicle, *TH* thalamus

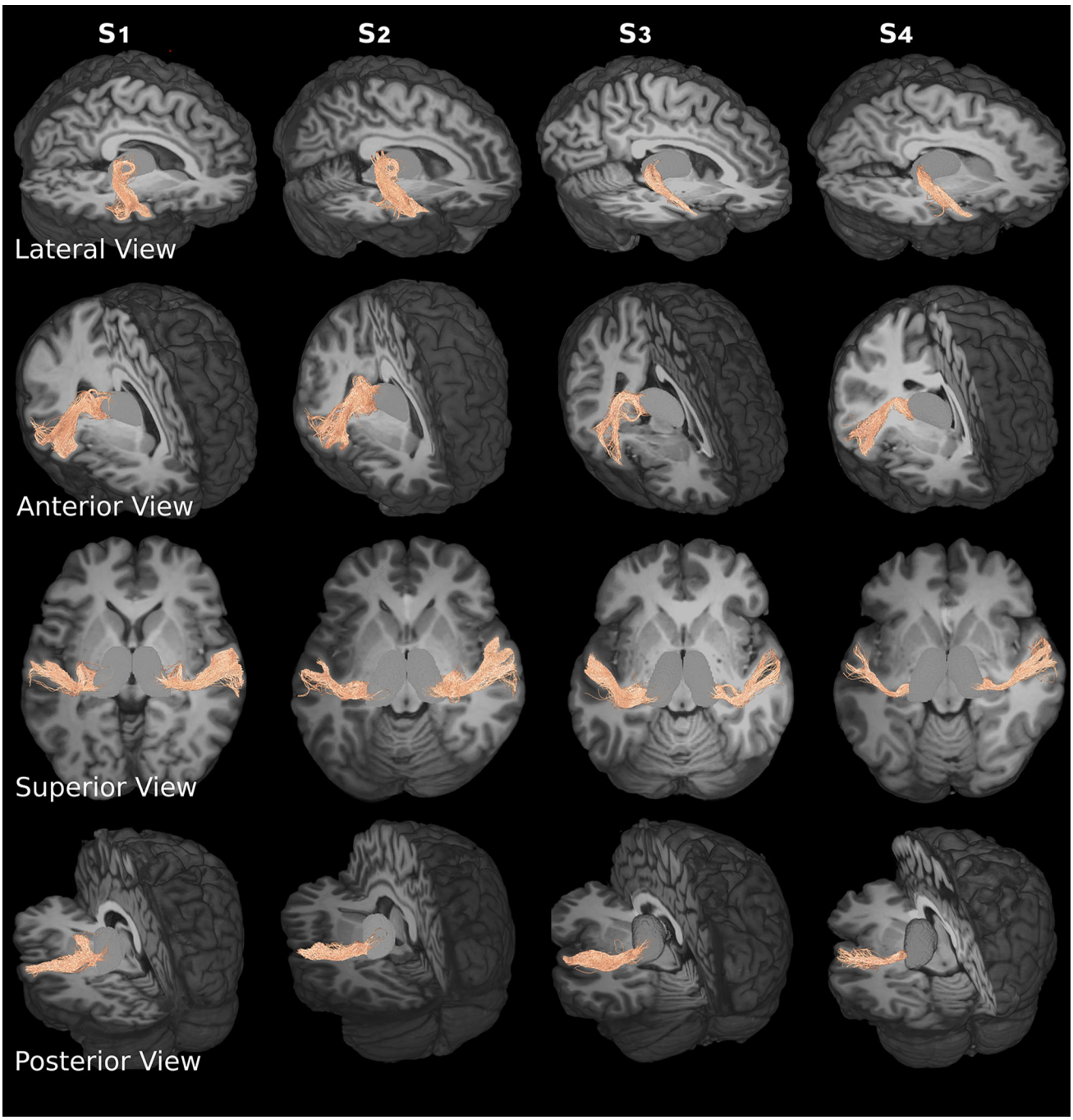

Fig. 4 3D reconstruction of the *right* and *left* AR in four healthy subjects (S1, S2, S3, and S4). The course of the AR is shown from *top* to *bottom rows* in lateral, anterior, superior, and posterior views. The tractography reconstruction is overlaid on the corresponding T1 anatomical scan of each subject. *AR* acoustic radiation

Comparison of dissection and tractography results

Blunt micro-dissections and tractography show comparable results in the reconstruction of the AR profile. Both techniques show AR fibers stemming at the posterior lateral thalamus, moving lateral, arching around the posterior circular sulcus of the insula, moving antero-lateral, and terminating in the upper cortex of the posterior temporal lobe. However, notable differences between techniques are also visible, which highlight current limitations of diffusion tractography. At the level of the genu, where the AR crosses the IC fibers, some of the reconstructed streamlines follow erroneous vertical directions creating implausible false-positive artifacts (Supplementary Figure 1-a). At this

level, the dense fibers crossing makes also the blunt dissection very hard to perform, particularly in disentangling between the AR and the vertical thalamic fibers (Fig. 3d). At the fan level, while blunt micro-dissections clearly highlighted the core of termination of AR at the level of HG, the 3D tractography reconstruction was quite noisy in most of the subjects, and some streamlines did not stop in HG, but continued outside the gyral borders in the antero-posterior direction (Supplementary Figure 1-b). This artifact was less visible when tractography was initiated in the HG and the thalamus was targeted. However, in this case, tractography was noisier at the thalamus, where many false-positive artifacts were visible (Supplementary Figure 2). Overall, reverse seeding does not seem to improve the AR reconstruction, particularly at the level of the crossing with the vertical thalamic fibers, where the same artifacts are visible.

Discussion

To the best of our knowledge, this is the first study revealing the anatomical features and topography of the AR in the human brain to combine ex vivo (blunt micro-dissections) and in vivo (diffusion tractography) data. Both methods showed the unique transversal trajectory of the AR running from the midline to the lateral convexity of the posterior portion of the superior temporal lobe. No other anatomical structure with the same orientation has been described in this region, excluding bi-hemispherical connections of the corpus callosum in human (Westerhausen et al. 2009) and non-human primates (Schmahmann and Pandya 2006). For this reason, over its course from the thalamus to the HG, the AR crosses several association and projection bundles.

Near the genu (proximal portion) of the AR, after the emergence from the MGN, these fibers cross in a medio-lateral direction a compact layer of vertical thalamo-cortical fibers. Intermingling this thick and compact wall, AR fibers form a highly-organized structure at the level of the stem. Here, these cross medio-laterally with the peri-sylvian association pathways, with a prevalent antero-posterior horizontal course. In the genu and stem portions, the AR is in close proximity of PTR, OR, EC, claustro-opercular fibers (genu), AF, and indirect anterior SLF (stem). Even at the termination site (HG), these fibers are adjacent to the terminations of different and multi-directional associative pathways (e.g., AF, SLF, etc.).

The complex fiber architecture of this region, with a high density of crossing, kissing, and bending fibers, represents an open challenge for diffusion-based tractography techniques (Dell'Acqua and Catani 2012). We show that using high angular resolution multi-shell HCP data and CSD-based probabilistic tractography, it is possible to reconstruct the profile of the AR bundle with results comparable to blunt dissections. However, when compared with ex vivo results, 3D tractography reconstructions of the AR from diffusion MR data still present with two main limitations: at the level of the crossing with the thalamic cortical fibers, some AR streamlines are likely to be truncated or may follow incorrect vertical directions, creating false-positive artifacts; at the cortical termination site in HG, the accuracy of the tractography may be suboptimal, with some streamlines that rather than stopping in HG continue outside the gyral borders in the antero-posterior direction along the cortex. Lack of precision in determining streamlines terminations at the cortex constitutes a limit in diffusion-based tractography techniques. When tracking, macroscopic termination criteria are used (e.g., white matter binary mask; edge of the brain, white matter–gray matter interface) that are inherently affected by limits in spatial resolution, partial volume effects and noise. As a result, streamlines endpoints not necessarily reflect the endpoints of the tracts (Alexander and Barker 2005; Schmahmann and Pandya 2006; Jbabdi and Johansen-Berg 2011). When tractography is performed in the opposite direction (latero-medial), the same artifacts are visible at the thalamus, with streamlines exiting its borders. More investigation is needed to understand if a combination of the two, or the implementation of better termination strategies, would help to obtain more precise 3D reconstructions of the AR.

Solving the crossing between the AR and the compact vertical thalamic fibers represents the main obstacle in attempts at AR reconstruction using tractography methods. Most of the available clinical diffusion protocols and tractography pipelines may not be able to solve this, resulting in the AR being absent from the final reconstruction. The use of probabilistic tractography may help to overcome some of the limitations related to the diffusion model or tractography algorithm (Behrens et al. 2007; Descoteaux et al. 2009). However, these methods are also more prone to false-positive artifacts than deterministic ones. Being aware of the exact anatomical borders of the bundle, as highlighted by blunt dissections, is a crucial requirement for the interpretation of tractography results and for excluding non-reliable reconstructions. Most of the studies investigating the auditory pathways in healthy subjects and patients used ROI-based analysis to extract DTI quantitative measures from atlas-derived regions of interest (Chang et al. 2004; Lee et al. 2007; Lin et al. 2008). However, these masks can lead to very inaccurate results, particularly for WM tracts that are extremely variable across subjects (Rademacher et al. 2002). It is thus highly preferable to map the exact anatomy in individual subjects/patients.

Reliable in vivo reconstruction of the AR would help to shed a light on the mechanisms underlying auditory and language comprehension in humans. The anatomical and topographical description of the AR that emerged from this study may reflect the anatomo-functional link between auditory sensorial input and language elaboration, especially considering the close proximity of the AR terminations with the major language bundles of the dorsal perisylvian network at the junction between the posterior temporal lobe and inferior parietal lobule (a crucial hub for semantic and articulatory/phonological integration). In the widely accepted dual streams model of language processing (Hickok and Poeppel 2007; Saur et al. 2008), the AF/SLF system is considered the anatomical structure mediating the elaboration of auditory inputs, before this is passed to the auditory-motor interface for speech processing (Catani et al. 2005; Duffau et al. 2014). This auditory information is brought into the system via the fibers of the AR. In this highly-integrated and distributed network, an appreciation of the structural neuroanatomy is crucial for the comprehension of the different steps of processing between sensory perception and conceptual representations (Hickok and Poeppel 2004). Investigating the functional substrates of this structure will help understand the degree of linguistic specificity of the AR and auditory territories. Current theories assume that the auditory stimulus is computed asymmetrically even at very early stages, with the left hemisphere being specialized in processing fast temporal changes that are not language specific, but are indispensable for speech processing, and the right hemisphere being specialized in spectral analysis that might be more important for music perception (Zatorre et al. 2002). Disentangling the role of the AR pathways in speech processing and music perception would be particular relevant, for example, in syndromes in which the level of language specificity of the deficit is still unclear, such as pure word deafness (Saffran et al. 1976; Stefanatos et al. 2005). In this scenario and considering also the evolution of brain surgery towards functional tailored resections, the anatomy of the AR is even more crucial for the most complete surgical planning, to avoid functional impairments in domains involving auditory processing (e.g., language, music, etc.). Investigating the functional substrates of this structure will help understand the degree of linguistic specificity of the AR and auditory territories.

In conclusion, combining blunt micro-dissections and diffusion-based tractography allows for the precise topography of the AR to be delineated. This will be crucial in the guidance of reconstruction and in evaluating the reliability of tractography dissection of this structure. Finally, the neuroanatomical organization of this pathway as showed in this study suggests how primary auditory processing may be integrated with high-level linguistic and non-linguistic cognitive processing. This may provide new directions for research into linguistic processing, with clinical relevance for the interpretation of symptoms, the improvement of treatments, and the surgical preservation of a fundamental sensory function of the human being.

Acknowledgements We are grateful to Andrea Anderle, nurse and artist, for his artwork illustrating the course and main relationships of acoustic radiation as emerged by micro-dissection and tractography.

References

Alexander DC, Barker GJ (2005) Optimal imaging parameters for fiber-orientation estimation in diffusion MRI. Neuroimage 27:357–367. doi:10.1016/j.neuroimage.2005.04.008

Basser PJ, Mattiello J, LeBihan D (1994) MR diffusion tensor spectroscopy and imaging. Biophys J 66:259–267. doi:10.1016/S0006-3495(94)80775-1

Behrens TEJ, Berg HJ, Jbabdi S, Rushworth MFS, Woolrich MW (2007) Probabilistic diffusion tractography with multiple fibre orientations: what can we gain? Neuroimage 34:144–155. doi:10.1016/j.neuroimage.2006.09.018

Berman JI, Lanza MR, Blaskey L, Edgar JC, Roberts TPL (2013) High angular resolution diffusion imaging probabilistic tractography of the auditory radiation. Am J Neuroradiol 34:1573–1578. doi:10.3174/ajnr.A3471

Bürgel U, Amunts K, Hoemke L, Mohlberg H, Gilsbach JM, Zilles K (2006) White matter fiber tracts of the human brain: three-dimensional mapping at microscopic resolution, topography and intersubject variability. Neuroimage 29:1092–1105. doi:10.1016/j.neuroimage.2005.08.040

Catani M, Howard RJ, Pajevic S, Jones DK (2002) Virtual in vivo interactive dissection of white matter fasciculi in the human brain. Neuroimage 17:77–94. doi:10.1006/nimg.2002.1136

Catani M, Jones DK, Donato R, Ffytche DH (2003) Occipito-temporal connections in the human brain. Brain 126:2093–2107. doi:10.1093/brain/awg203

Catani M, Jones DK, Ffytche DH (2005) Perisylvian language networks of the human brain. Ann Neurol 57:8–16. doi:10.1002/ana.20319

Chamberland M, Whittingstall K, Fortin D, Mathieu D, Descoteaux M (2014) Real-time multi-peak tractography for instantaneous connectivity display. Front Neuroinform 8:1–15. doi:10.3389/fninf.2014.00059

Chang Y, Lee SH, Lee YJ, Hwang MJ, Bae SJ, Kim MN, Kang DS (2004) Auditory neural pathway evaluation on sensorineural hearing loss using diffusion tensor imaging. NeuroReport 15(11):1699–1703

Crippa A, Lanting CP, van Dijk P, Roerdink JBTM (2010) A diffusion tensor imaging study on the auditory system and tinnitus. Open Neuroimaging J 4:16–25. doi:10.2174/1874440001004010016

De Benedictis A, Petit L, Descoteaux M, Marras CE, Barbareschi M, Corsini F, Dallabona M, Chioffi F, Sarubbo S (2016) New insights in the homotopic and heterotopic connectivity of the frontal portion of the human corpus callosum revealed by microdissection and diffusion tractography. Hum Brain Mapp 37:4718–4735. doi:10.1002/hbm.23339

Dejerine J (1895) Anatomie des Centres Nerveux. Reuff, Paris

Dell'Acqua F, Catani M (2012) Structural human brain networks: hot topics in diffusion tractography. Curr Opin Neurol 25:375–383. doi:10.1097/WCO.0b013e328355d544

Dell'Acqua F, Scifo P, Rizzo G, Catani M, Simmons A, Scotti G, Fazio F (2010) A modified damped Richardson–Lucy algorithm to reduce isotropic background effects in spherical deconvolution. Neuroimage 49:1446–1458. doi:10.1016/j.neuroimage.2009.09.033

Descoteaux M, Deriche R, Knosche T, Anwander A (2009) Deterministic and probabilistic tractography based on complex fiber orientation distribution. IEEE Trans Med Imaging 28:269–286

Duffau H, Moritz-Gasser S, Mandonnet E (2014) A re-examination of neural basis of language processing: proposal of a dynamic hodotopical model from data provided by brain stimulation mapping during picture naming. Brain Lang 131:1–10. doi:10.1016/j.bandl.2013.05.011

Fan Q, Witzel T, Nummenmaa A, Van Dijk KRA, Van Horn JD, Drews MK, Somerville LH, Sheridan MA, Santillana RM, Snyder J, Hedden T, Shaw EE, Hollinshead MO, Renvall V, Zanzonico R, Keil B, Cauley S, Polimeni JR, Tisdall D, Buckner RL, Wedeen VJ, Wald LL, Toga AW, Rosen BR (2015) MGH-USC Human Connectome Project datasets with ultra-high *b*-value diffusion MRI. Neuroimage. doi:10.1016/j.neuroimage.2015.08.075

Fernández-Miranda JC, Wang Y, Pathak S, Stefaneau L, Verstynen T, Yeh F-C (2015) Asymmetry, connectivity, and segmentation of the arcuate fascicle in the human brain. Brain Struct Funct 220:1665–1680. doi:10.1007/s00429-014-0751-7

Flechsig P (1920) Anatomie des menschlichen Gehirns und Ruckenmarks auf myellogenetischer Grundlage. Erster Band, Georg Thieme Verlag, Leipzig

Hackett TA, Stepniewska I, Kaas JH (1998) Thalamocortical connections of the parabelt auditory cortex in macaque monkeys. J Comp Neurol 400:271–286

Hickok G, Poeppel D (2004) Dorsal and ventral streams: a framework for understanding aspects of the functional anatomy of language. Cognition 92:67–99. doi:10.1016/j.cognition.2003.10.011

Hickok G, Poeppel D (2007) The cortical organization of speech processing. Nat Rev Neurosci 8:393–402. doi:10.1038/nrn2113

Javad F, Warren JD, Micallef C, Thornton JS, Golay X, Yousry T, Mancini L (2014) Auditory tracts identified with combined fMRI and diffusion tractography. Neuroimage 84:562–574. doi:10.1016/j.neuroimage.2013.09.007

Jbabdi S, Johansen-Berg H (2011) Tractography: where do we go from here? Brain Connect 1(3):169–183

Jeurissen B, Leemans A, Tournier JD, Jones DK, Sijbers J (2013) Investigating the prevalence of complex fiber configurations in white matter tissue with diffusion magnetic resonance imaging. Hum Brain Mapp 34:2747–2766. doi:10.1002/hbm.22099

Jeurissen B, Tournier J-D, Dhollander T, Connelly A, Sijbers J (2014) Multi-tissue constrained spherical deconvolution for improved analysis of multi-shell diffusion MRI data. Neuroimage 103:411–426. doi:10.1016/j.neuroimage.2014.07.061

Jones DK, Cercignani M (2010) Twenty-five pitfalls in the analysis of diffusion MRI data. NMR Biomed 23:803–820. doi:10.1002/nbm.1543

Klein A, Andersson J, Ardekani BA, Ashburner J, Avants B, Chiang M-C, Christensen GE, Collins DL, Gee J, Hellier P, Song JH, Jenkinson M, Lepage C, Rueckert D, Thompson P, Vercauteren T, Woods RP, Mann JJ, Parsey RV (2009) Evaluation of 14 nonlinear deformation algorithms applied to human brain MRI registration. Neuroimage 46:786–802. doi:10.1016/j.neuroimage.2008.12.037

Lee YJ, Bae SJ, Lee SH, Lee JJ, Lee KY, Kim MN, Kim YS, Baik SK, Woo S, Chang Y (2007) Evaluation of white matter structures in patients with tinnitus using diffusion tensor imaging. J Clin Neurosci 14:515–519. doi:10.1016/j.jocn.2006.10.002

Lin Y, Wang J, Wu C, Wai Y, Yu J, Ng S (2008) Diffusion tensor imaging of the auditory pathway in sensorineural hearing loss: changes in radial diffusivity and diffusion anisotropy. J Magn Reson Imaging 28(3):598–603

Maffei C, Soria G, Prats-Galino A, Catani M (2015) Imaging white-matter pathways of the auditory system with diffusion imaging tractography. In: Celesia GG, Hickok G (eds) The human auditory system: fundamental organization and clinical disorders. Elsevier Inc., Amsterdam

Martino J, Vergani F, Robles SG, Duffau H (2010) New insights into the anatomic dissection of the temporal stem with special emphasis on the inferior fronto-occipital fasciculus. Oper Neurosurg 66:4–12. doi:10.1227/01.NEU.0000348564.28415

Mesulam MM, Pandya DN (1973) The projections of the medial geniculate complex within the sylvian fissure of the rhesus monkey. Brain Res 60:315–333

Patenaude B, Smith SM, Kennedy D, Jenkinson M (2012) A Bayesian model of shape and appearance for subcortical brain segmentation. Neuroimage 56:907–922. doi:10.1016/j.neuroimage.2011.02.046

Pfeifer R (1920) Myelogenetisch-anatomische Untersuchungen uber das kortikale Ende der Horleitung. Abh Math Phys Kl Sachs Akad Wiss 37:1–54

Poeppel D, Emmorey K, Hickok G, Pylkkänen L (2012) Towards a new neurobiology of language. J Neurosci 32:14125–14131. doi:10.1523/JNEUROSCI.3244-12.2012

Rademacher J, Bürgel U, Zilles K (2002) Stereotaxic localization, intersubject variability, and interhemispheric differences of the human auditory thalamocortical system. Neuroimage 17:142–160

Saffran EM, Marin OS, Yeni-Komshian GH (1976) An analysis of speech perception in word deafness. Brain Lang 3:209–228

Sarubbo S, De Benedictis A, Milani P, Paradiso B, Barbareschi M, Rozzanigo U, Colarusso E, Tugnoli V, Farneti M, Granieri E, Duffau H, Chioffi F (2015) The course and the anatomo-functional relationships of the optic radiation: a combined study with "post mortem" dissections and "in vivo" direct electrical mapping. J Anat 226:47–59. doi:10.1111/joa.12254

Sarubbo S, De Benedictis A, Merler S, Mandonnet E, Barbareschi M, Dallabona M, Chioffi F, Duffau H (2016) Structural and functional integration between dorsal and ventral language streams as revealed by blunt dissection and direct electrical stimulation. Hum Brain Mapp 37:3858–3872. doi:10.1002/hbm.23281

Saur D, Kreher BW, Schnell S, Kümmerer D, Kellmeyer P, Vry M-S, Umarova R, Musso M, Glauche V, Abel S, Huber W, Rijntjes M, Hennig J, Weiller C (2008) Ventral and dorsal pathways for language. Proc Natl Acad Sci USA 105:18035–18040. doi:10.1073/pnas.0805234105

Schmahmann J, Pandya D (2006) Fiber pathways of the brain. Oxford University Press, Oxford

Smith RE, Tournier J-D, Calamante F, Connelly A (2012) Anatomically-constrained tractography: improved diffusion MRI streamlines tractography through effective use of anatomical information. Neuroimage 62:1924–1938. doi:10.1016/j.neuroimage.2012.06.005

Stefanatos GA, Gershkoff A, Madigan S (2005) On pure word deafness, temporal processing, and the left hemisphere. J Int Neuropsychol Soc 11:456–470

Tardif E, Clarke S (2001) Intrinsic connectivity of human auditory areas: a tracing study with DiI. Eur J Neurosci 13:1045–1050

Thiebaut de Schotten M, Ffytche DH, Bizzi A, Dell'Acqua F, Allin M, Walshe M, Murray R, Williams SC, Murphy DGM, Catani M (2011) Atlasing location, asymmetry and inter-subject variability of white matter tracts in the human brain with MR diffusion

tractography. Neuroimage 54:49–59. doi:10.1016/j.neuroimage.2010.07.055

Tournier JD, Yeh CH, Calamante F, Cho KH, Connelly A, Lin CP (2008) Resolving crossing fibres using constrained spherical deconvolution: validation using diffusion-weighted imaging phantom data. Neuroimage 42:617–625. doi:10.1016/j.neuroimage.2008.05.002

Tournier J-D, Mori S, Leemans A (2011) Diffusion tensor imaging and beyond. Magn Reson Med 65:1532–1556. doi:10.1002/mrm.22924

Tournier JD, Calamante F, Connelly A (2012) MRtrix: diffusion tractography in crossing fiber regions. Int J Imaging Syst Technol 22:53–66. doi:10.1002/ima.22005

Wang Y, Fernandez-Miranda JC, Verstynen T, Pathak S, Schneider W, Yeh FC (2012) Rethinking the role of the middle longitudinal fascicle in language and auditory pathways. Cereb Cortex 23:2347–2356. doi:10.1093/cercor/bhs225

Wang X, Pathak S, Stefaneanu L, Yeh F-C, Li S, Fernandez-Miranda JC (2016) Subcomponents and connectivity of the superior longitudinal fasciculus in the human brain. Brain Struct Funct 221:2075–2092. doi:10.1007/s00429-015-1028-5

Westerhausen R, Gruner R, Specht K, Hugdahl K (2009) Functional relevance of interindividual differences in temporal lobe callosal pathways: a DTI tractography study. Cereb Cortex 19:1322–1329. doi:10.1093/cercor/bhn173

Zatorre RJ, Belin P, Penhune VB (2002) Structure and function of auditory cortex: music and speech. Trends Cogn Sci 6:37–46

Zhang Y, Brady M, Smith S (2001) Segmentation of brain MR images through a hidden markov random field model and the expectation-maximization algorithm 20:45–57